Magnetic Discontinuities in the Near-Earth Solar Wind: Evidence of In-Transit Turbulence or Remnants of Coronal Structure?

Solar Physics
A Journal for Solar and Solar-Stellar Research and the Study of Solar Terrestrial Physics

ISSN 0038-0938
Volume 269
Number 2

Sol Phys (2011) 269:411-420
DOI 10.1007/
s11207-010-9695-0

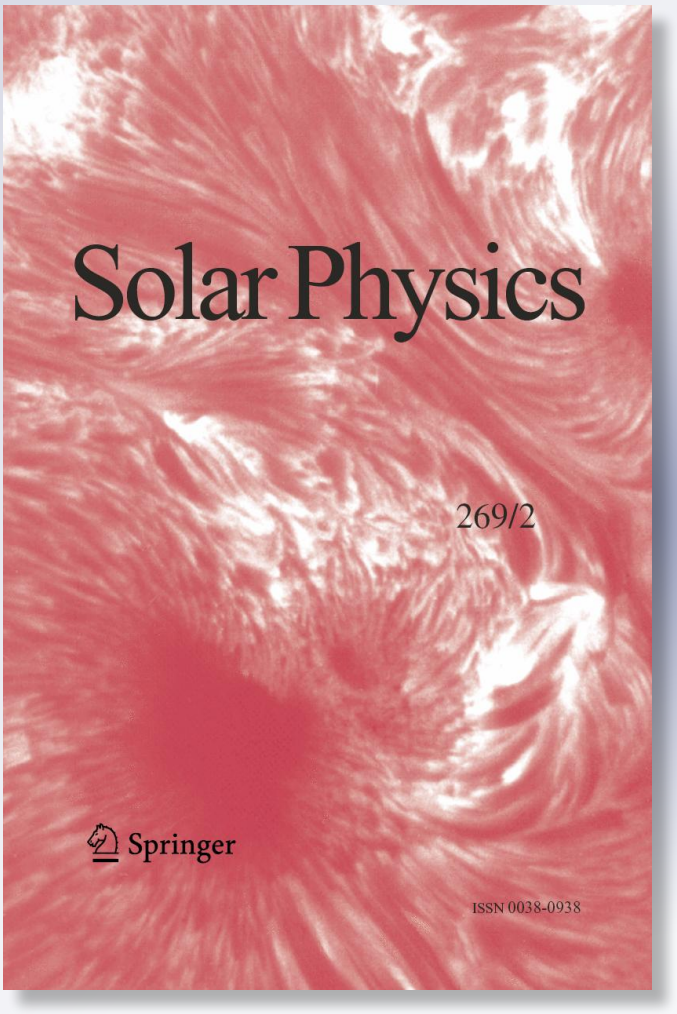

Springer

Solar Phys (2011) 269: 411–420
DOI 10.1007/s11207-010-9695-0

Magnetic Discontinuities in the Near-Earth Solar Wind: Evidence of In-Transit Turbulence or Remnants of Coronal Structure?

M.J. Owens · R.T. Wicks · T.S. Horbury

Received: 15 July 2010 / Accepted: 30 November 2010 / Published online: 1 January 2011

Abstract Fluctuations in the solar wind plasma and magnetic field are well described by the sum of two power law distributions. It has been postulated that these distributions are the result of two independent processes: turbulence, which contributes mainly to the smaller fluctuations, and crossing the boundaries of flux tubes of coronal origin, which dominates the larger variations. In this study we explore the correspondence between changes in the magnetic field with changes in other solar wind properties. Changes in density and temperature may result from either turbulence or coronal structures, whereas changes in composition, such as the alpha-to-proton ratio are unlikely to arise from in-transit effects. Observations spanning the entire ACE dataset are compared with a null hypothesis of no correlation between magnetic field discontinuities and changes in other solar wind parameters. Evidence for coronal structuring is weaker than for in-transit turbulence, with only $\sim 25\%$ of large magnetic field discontinuities associated with a significant change in the alpha-to-proton ratio, compared to $\sim 40\%$ for significant density and temperature changes. However, note that a lack of detectable alpha-to-proton signature is not sufficient to discount a structure as having a solar origin.

Keywords Coronal heating · Magnetic discontinuities · Solar wind · Solar wind turbulence

1. Introduction

Single-point spacecraft observations reveal fluctuations in the solar wind plasma and magnetic field over a wide range of time scales. These are interpreted as a combination of spatial and temporal variations in the rest frame of the plasma, with waves, shocks, turbulence and

M.J. Owens (✉)
Space Environment Physics Group, Department of Meteorology, University of Reading, Earley Gate, PO Box 243, Reading RG6 6BB, UK
e-mail: m.j.owens@reading.ac.uk

M.J. Owens · R.T. Wicks · T.S. Horbury
Space and Atmospheric Physics, Imperial College London, Prince Consort Road, London SW7 2AZ, UK

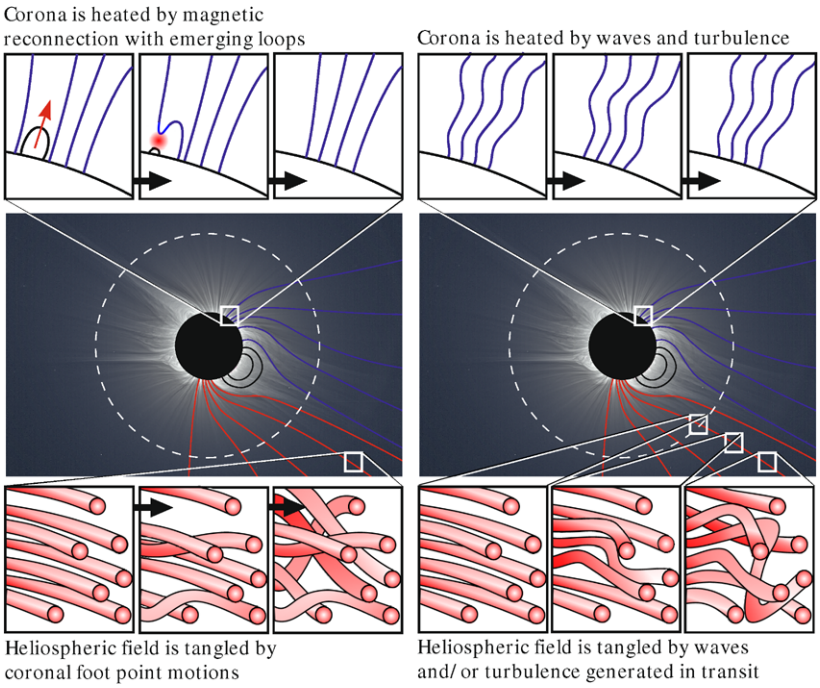

Figure 1 Sketches of two possible mechanisms for coronal heating and subsequent heliospheric magnetic field braiding. In the left-hand sketch, the corona is heated by reconnection between open solar flux and closed loops emerging through the photosphere. In this model, the heliospheric magnetic field is likely to become tangled due to foot point motions. In the right-hand sketch, the corona is heated by waves or turbulence. The heliospheric magnetic field can then become tangled by turbulent motions, either propagating directly from the corona or generated in transit.

tangential and rotational discontinuities all likely contributing (*e.g.*, Horbury *et al.*, 2001; Bruno *et al.*, 2001; Bruno and Carbone, 2005). It is of considerable interest to discern between fluctuations of turbulent or coronal origin, as this can provide a constraint on the physical mechanism(s) by which the corona is heated and the solar wind formed.

Figure 1 shows sketches of two possible mechanisms for coronal heating and their implications for heliospheric magnetic field discontinuities as structures convect over an observing spacecraft. Both models are able to produce fast and slow solar wind, as well as observed in situ composition signatures (Cranmer, 2008). In the left-hand sketch, the corona is heated by reconnection between open solar flux and closed loops emerging through the photosphere (see, *e.g.*, Fisk and Schwadron, 2001; Schwadron and McComas, 2003; Schwadron, McComas, and DeForest, 2006), and the heliospheric magnetic field will naturally become tangled due to foot point motions. In the right-hand sketch, the corona is heated by waves or turbulence (see, *e.g.*, Cranmer and van Ballegooijen, 2005; Verdini and Velli, 2007). The heliospheric magnetic field can then become tangled by turbulent motions, either propagating directly from the corona or generated in transit.

Borovsky (2008) showed that the observed occurrence rate of changes in the magnetic field direction at 1 AU ($\Delta\theta_B$) can be fit by assuming two distinct populations. It was suggested that periods of low $\Delta\theta_B$, *e.g.*, below 45°, can be attributed to turbulence, whereas larger $\Delta\theta_B$ intervals were explained in terms of crossing walls of magnetic flux tubes formed near the Sun. The occurrence rate of other solar wind parameters, including proton temper-

ature (T_P), density (n_P), and the alpha-to-proton ratio (α/p) were shown to exhibit a similar dual distribution.

Solar wind density and temperature are expected to undergo significant evolution during transit from the Sun to 1 AU, through both linear and non-linear processes. Conversely, elemental abundance, in particular the alpha-to-proton ratio, is primarily determined by coronal processes and is difficult to modify during the subsequent transit to the observer (Borrini *et al.*, 1981; Aellig, Lazarus, and Steinberg, 2001). Borovsky (2008) found that, for two years of *Advanced Composition Explorer* (ACE) measurements, α/p is typically higher for $\Delta\theta > 50°$ than $\Delta\theta < 15°$. This suggests that the largest changes in magnetic field direction may have a solar origin. Similarly, for intervals of periodic solar wind density fluctuations, Viall, Spence, and Kasper (2009) found an anti-correlation with α/p. However, the general interrelation between $\Delta\theta$ and $\Delta\alpha/p$, along with its statistical significance, has still to be fully investigated and is addressed in this study.

2. Data

ACE magnetic field data from the Magnetic Field Investigation (MFI, Smith *et al.*, 1998) and plasma data from the Solar Wind Electron Proton Alpha Monitor (SWEPAM, McComas *et al.*, 1998) are used at 64-second resolution, the spin period of the spacecraft. The data cover the whole of the available ACE mission, from January 1998 to June 2009. Periods during which no data are available are removed from the study (no interpolation is made), and only the time interval of 64 seconds is considered for the data. This results in approximately 3.5 million data points. No attempt is made to remove intervals associated with coronal mass ejections (CMEs) and corotating interaction regions (CIRs) from the time series. By treating the solar wind dataset as a whole, we assume that CMEs are merely the largest structures in a spectrum of coronal flux tubes (*e.g.*, half the solar wind magnetic flux at solar maximum may be the result of CMEs, Owens and Crooker, 2006).

For the whole dataset, we compute the fractional change in solar wind parameters between consecutive data points, D_X, for both vector (*i.e.*, magnetic field and plasma velocity) and scalar (*i.e.*, proton temperature, density and alpha-to-proton ratio) quantities:

$$D_X = \frac{\Delta \mathbf{X}}{\langle |\mathbf{X}| \rangle} = \frac{|\mathbf{X}_i - \mathbf{X}_{i+1}|}{|\mathbf{X}_i + \mathbf{X}_{i+1}|/2}. \tag{1}$$

Thus D_X is a scalar quantity regardless of whether X is a scalar or vector quantity. In order to aid direct comparison with the work of Borovsky (2008), we also consider the angular change in the magnetic field vector between consecutive data points, $\Delta\theta_B$.

3. Solar wind Variations

We consider the 64-second variations in solar wind parameters in three stages. First, the individual probability distribution functions (PDFs) are computed over the whole dataset. Next, the joint occurrence rates between solar wind parameters and changes in the magnetic field are investigated for any interrelation. Finally, the individual PDFs are combined to calculate the null hypothesis of no interrelation, which is compared with the observations.

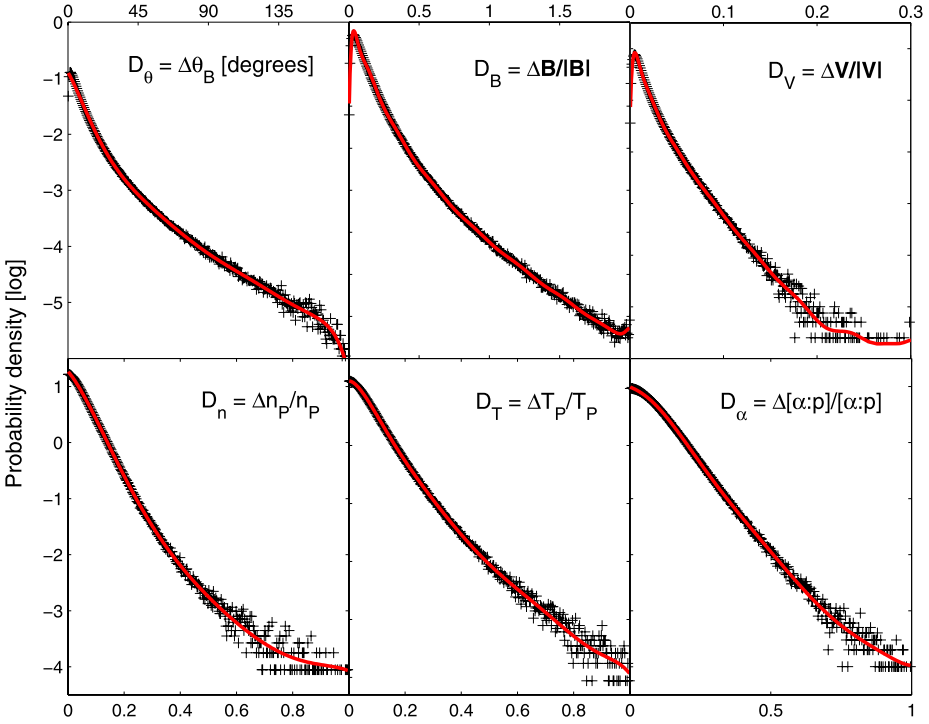

Figure 2 The individual PDFs for point-to-point changes in various solar wind parameters at 64-second resolution. D_{V} and D_{B} are the magnitude of changes in the vector velocity and magnetic field, respectively. D_n, D_{T} and D_α are changes in the scalar quantities of density, temperature and alpha-to-proton ratio, respectively. All data are shown on a logarithmic scale. The red lines are the best fits using a high-order polynomial function.

3.1. Individual Occurrence Rates

Figure 2 shows $P(D_X)$, the PDF of fractional changes in solar wind parameters. A logarithmic scale is used. The magnetic field vector, magnetic field angle, proton velocity vector, proton temperature, proton density and the alpha-to-proton ratio are all considered.

We do not attempt to draw any conclusions from these individual PDFs; in particular, no attempt is made to deconvolve them into component distributions. However, the red line shows the best fit to observed PDFs using a high-order ($n = 10$) polynomial function which is used to analytically characterise the PDFs to compute the null hypothesis in Section 3.3.

3.2. Joint Occurrence Rates

While changes in solar wind magnetic field and plasma properties have been described by two populations (Borovsky, 2008), it has not been explicitly established that large/small changes in one parameter are associated with large/small changes in another. Figure 3 shows changes in solar wind velocity, density, temperature and alpha-to-proton ratio binned by the associated changes in the magnetic field (in terms of both vector and angular changes).

Velocity variations dramatically increase with changes in the magnetic field, as expected for Alfvenic fluctuations, but with a possible decline at very large field changes. However,

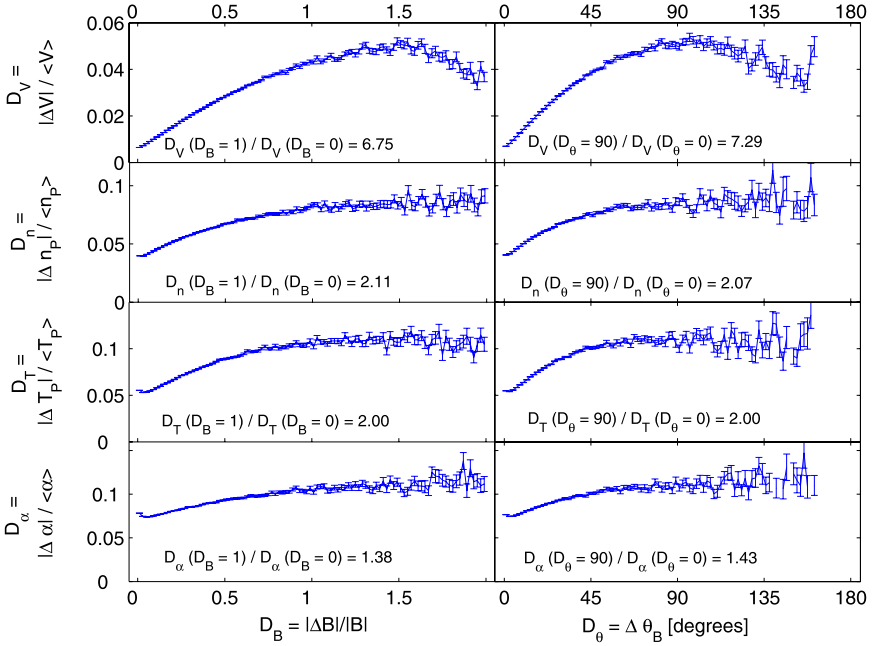

Figure 3 Changes in solar wind velocity, density, temperature and alpha-to-proton ratio binned by associated changes in the magnetic field (in terms of both vector and angular changes). The variation in alpha-to-proton ratio with the magnetic field is far less pronounced than the equivalent changes in solar wind velocity, density or temperature.

the uncertainties in the mean values of such extreme changes are largely due to the exponential decrease in occurrence rate (see, *e.g.*, Figure 2). Changes in solar wind density, temperature and alpha-to-proton ratio all steadily increase with magnetic field changes up to $D_{\mathrm{B}} \sim 1$ ($D_\theta \sim 90°$), after which they appear to plateau. Again, uncertainties at $D_{\mathrm{B}} > 1$ ($D_\theta > 90°$) are too large for us to draw firm conclusions about the interrelation between parameters in this regime.

The ratio of D_X at $D_{\mathrm{B}} = 1$ ($D_\theta = 90°$) to D_X at $D_{\mathrm{B}} = 0$ ($D_\theta = 0°$), shown in each panel of Figure 3, quantifies the interdependence of changes in a solar wind parameter with the magnetic field. Note that the change in D_α with magnetic field is significantly lower than the equivalent changes in solar wind velocity, density and temperature.

The mean value of D_X in the range $0° \geq D_\theta < 5°$ is the level of fluctuation in a solar wind property X when the magnetic field is effectively constant. We refer to this as the ambient fluctuation level in X. We consider a "significant" change in X to be one standard deviation above the ambient level. Figure 4 shows the fraction of changes in solar wind properties which meet this 'significant' criterion as the magnetic field variation increases. Large magnetic field changes (*e.g.*, $D_\theta \geq 90°$) are accompanied by significant velocity changes $\sim$85% of the time. The correspondence between large magnetic field changes and significant temperature and density changes is not as high, occurring $\sim$40% of the time. Significant changes in the alpha-to-proton ratio are only observed in conjunction with $\sim$25% of large magnetic field changes. If different "significance" criteria are used, *e.g.*, two standard deviations about the ambient fluctuation level, these numbers obviously change, but the overall trends shown in Figure 4 remain.

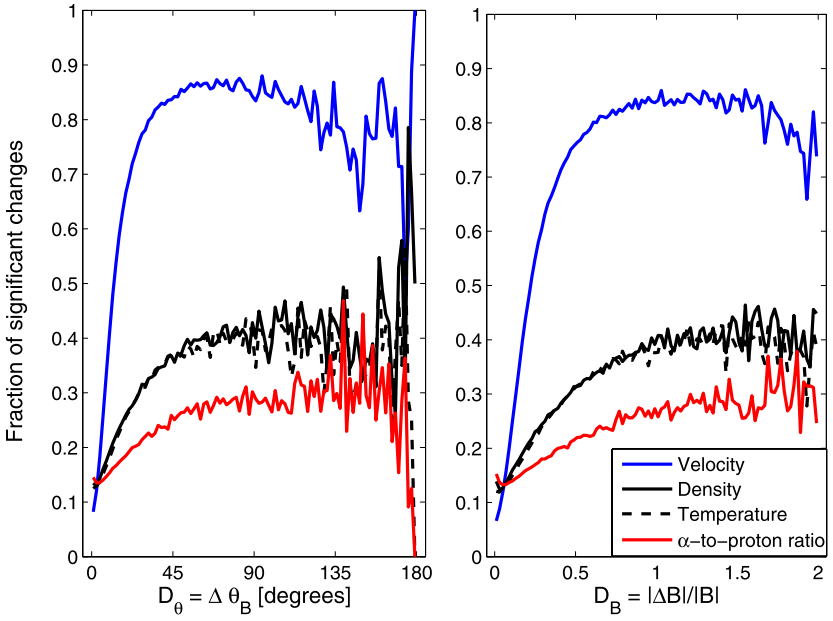

Figure 4 The fraction of "significant" changes in solar wind properties associated with increasing magnetic field variations. Large magnetic field changes (*e.g.*, $D_\theta \geq 90°$) are accompanied by significant velocity changes ∼85% of the time. The correspondence between large magnetic field changes and significant temperature and density changes is not as high, occurring ∼40% of the time. Significant changes in the alpha-to-proton ratio are only observed in conjunction with ∼25% of large magnetic field changes.

3.3. Occurrence Rates Above the Null Hypothesis

Such mean values (and associated measures like correlation coefficients) may not be good measures of the interrelation between solar wind parameters, as the distribution functions are heavily skewed towards small changes (*e.g.*, see Figure 2). For this reason, we compare the observed joint distributions of parameters with a null hypothesis that those parameters vary completely independently. The probability distribution of the null hypothesis is given by

$$P_{\mathrm{NULL}}(D_X, D_Y) = P(D_X)P(D_Y), \tag{2}$$

where $P(D_X)$ and $P(D_Y)$ are the independent PDFs established in Section 3.1 by the best fits to the observations (the red lines in Figure 2).

We also compute the observed joint probability distribution, $P_{\mathrm{OBS}}(D_X, D_Y)$. This is the normalised two-dimensional histogram of D_X and D_Y, *i.e.*, the number of data points in the interval D_X and $D_X + \Delta D_X$, and D_Y and $D_Y + \Delta D_Y$, divided by the total number of points. ΔD_X and ΔD_Y are chosen to give 40 equally spaced bins over the whole range of D_X and D_Y. Any bin with fewer than 100 data points is discarded from the analysis.

To illustrate this method, we first consider the relation between point-to-point changes in the magnetic field vector, D_{B}, and changes in the proton temperature, D_{T}. The left-hand panel of Figure 5 shows the probability density of the null hypothesis, $P_{\mathrm{NULL}}(D_{\mathrm{B}}, D_{\mathrm{T}})$, wherein temperature and magnetic field vector vary completely independently. This is con-

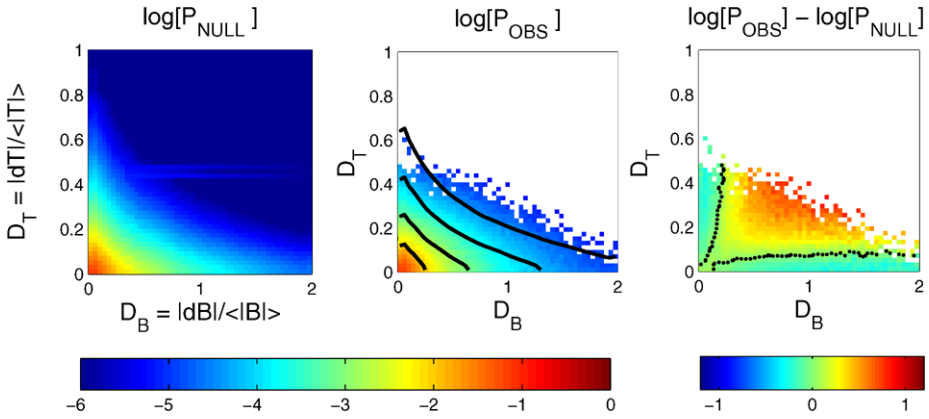

Figure 5 The relation between changes in proton temperature and magnetic field vector. Left: P_{NULL}, the probability density of the null hypothesis, wherein temperature and magnetic field vector vary completely independently. This is constructed from the individual PDFs shown in Figure 2. A logarithmic colour scale is used. Centre: P_{OBS}, the observed joint probability density of changes in temperature and magnetic field vector, on the same colour scale. Contours of P_{NULL} are shown as black lines. Right: The difference between the logs of P_{OBS} and P_{NULL}. Red (blue) indicates more (fewer) observations than expected if the variables were independent. There is a clear correlation between field and temperature changes.

structed from the observed individual PDFs shown in Figure 2. A log colour scale is used. The middle panel shows the observed joint distribution, $P_{\mathrm{OBS}}(D_{\mathrm{B}}, D_{\mathrm{T}})$, on the same scale. Contours of $P_{\mathrm{NULL}}(D_{\mathrm{B}}, D_{\mathrm{T}})$ are over-plotted in black. Finally, the right-hand panel of Figure 5 shows $\log[P_{\mathrm{OBS}}] - \log[P_{\mathrm{NULL}}]$, with red (blue) showing a greater (lesser) number of points observed than expected from independent variations. Black dots show the contour of $P_{\mathrm{NULL}} = P_{\mathrm{OBS}}$. Compared with the null hypothesis, there is an over-abundance of small (large) temperature changes associated with small (large) magnetic field changes. Conversely, there is a paucity of small temperature changes associated with large magnetic field changes, and vice versa. This implies a correlation between D_{B} and D_{T} at a level above the null hypothesis.

Figure 6 summarises the differences between the observed distributions and those expected from the null hypothesis for solar wind velocity, density, temperature and alpha-to-proton ratio. Red (blue) regions show a greater (lesser) number of observed points than would be expected from independent variables. The top two panels compare the change in the velocity vector with changes in the magnetic field vector (left) and angle (right). As expected from the highly Alfvenic nature of the solar wind, changes in the plasma velocity and magnetic field are highly correlated. There are also strong correlations between changes in magnetic field and density, and changes in magnetic field and temperature. Changes in the alpha-to-proton ratio are more weakly correlated with changes in the magnetic field, though still above the null hypothesis of independently varying parameters.

As a measure of the deviation of the observed distribution from the null hypothesis, we compute the mean deviation from the null hypothesis, $\lambda = \langle |\log(P_{\mathrm{OBS}}) - \log(P_{\mathrm{NULL}})| \rangle$; this is related to the mutual information of the distributions (see, *e.g.,* Wicks, Chapman, and Dendy, 2009). As seen by eye, λ is much higher for density and temperature than alpha-to-proton variations with magnetic field, thus quantifying the degree to which the observed distributions are correlated above the null hypothesis.

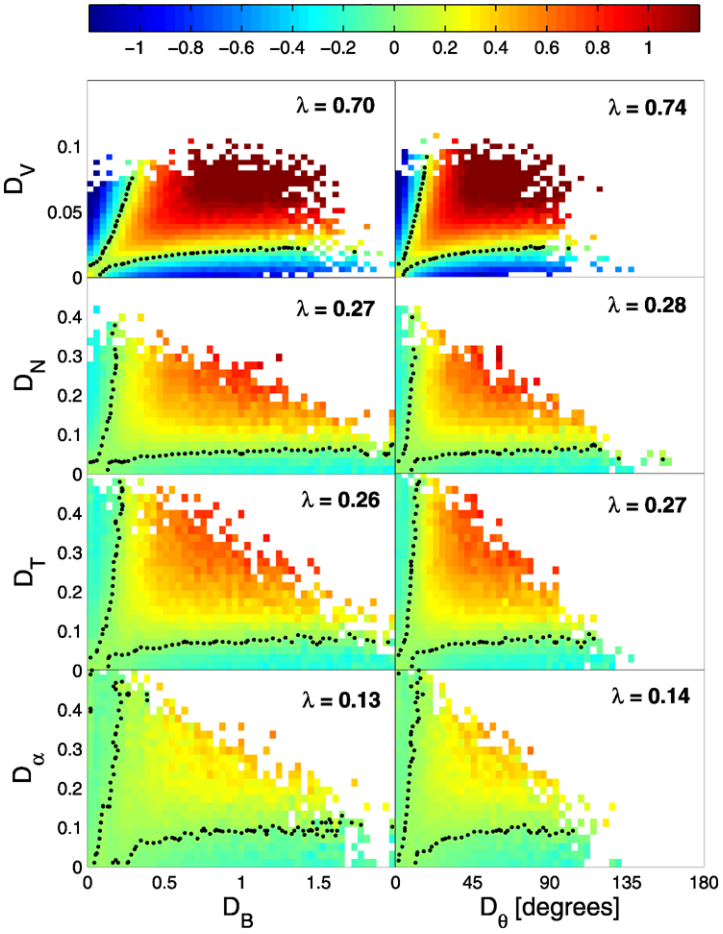

Figure 6 The deviation of the observed PDFs from the null hypothesis (*i.e.*, $\log[P_{\mathrm{OBS}}] - \log[P_{\mathrm{NULL}}]$) for various solar wind parameters. Red (blue) regions show a greater (lesser) number of observed points than expected from independent variations. Changes in the magnetic field and velocity vectors (the top two panels) are highly correlated due to the Alfvenic nature of the solar wind. There are also strong correlations between changes in magnetic field and density, and changes in magnetic field and temperature. Changes in the alpha-to-proton ratio are weakly correlated with changes in the magnetic field, though still above the null hypothesis.

4. Discussion

In this study we extended the Borovsky (2008) analysis of the occurrence rate of changes in solar wind properties to cover the whole ACE dataset. The correspondence between average changes in solar wind velocity, density and temperature with magnetic field was found to be much greater than that between the alpha-to-proton ratio and the magnetic field. Similarly, large magnetic field changes are associated with significant changes in velocity, density, temperature and alpha-to-proton ratio 85, 40, 40 and 25% of the time, respectively. By comparing with a null hypothesis, changes in velocity, density and temperature were found to correlate with changes in the magnetic field vector, well above the occurrence rate expected for independent variations. The correlation between changes in the alpha-to-proton ratio and

the magnetic field vector was weaker, though still significantly above the level expected for independent variations.

If we assume that density and temperature variations can be the result of either coronal structure or in-transit turbulence, whereas alpha-to-proton ratio variations are exclusively the result of changing coronal source, then our conclusions are largely in agreement with those of Borovsky (2008) and Viall, Spence, and Kasper (2009): Only a small subset of magnetic field discontinuities have an observable signature of changing coronal source. However, note that a lack of detectable alpha-to-proton signature is not sufficient to discount a structure as having a solar origin.

We have also investigated the occurrence rate of solar wind variations across magnetic field discontinuities with differing orientations at 1 AU. The results are not shown here, but changes in solar wind parameters across discontinuities perpendicular and parallel to the nominal Parker spiral direction were found to have nearly identical PDFs. Such isotropy also favours a dominance of in-transit turbulence over coronal structure, as the latter would be expected to become aligned with the underlying spiral field by the time the solar wind reaches 1 AU.

Finally we note that energetic particles, be they of solar, Jovian or galactic origin, may provide a means of tracing magnetic topology (see, *e.g.*, Owens, Horbury, and Arge, 2010), thus leading to further information about the nature of magnetic discontinuities in the solar wind. The analysis of such data will form the basis of future study.

Acknowledgements This research at Imperial College London was funded by STFC (UK). We are grateful for the availability of ACE magnetic field (P.I. Dr. C. Smith) and plasma (P.I. Dr. D. McComas) data.

References

Aellig, M.R., Lazarus, A.J., Steinberg, J.T.: 2001, The solar wind helium abundance: variation with wind speed and the solar cycle. *Geophys. Res. Lett.* **28**, 2767 – 2770. doi:10.1029/2000GL012771.

Borovsky, J.E.: 2008, Flux tube texture of the solar wind: strands of the magnetic carpet at 1 AU? *J. Geophys. Res.* **113**, 8110. doi:10.1029/2007JA012684.

Borrini, G., Wilcox, J.M., Gosling, J.T., Bame, S.J., Feldman, W.C.: 1981, Solar wind helium and hydrogen structure near the heliospheric current sheet – a signal of coronal streamers at 1 AU. *J. Geophys. Res.* **86**, 4565 – 4573. doi:10.1029/JA086iA06p04565.

Bruno, R., Carbone, V.: 2005, The solar wind as a turbulence laboratory. *Living Rev. Solar Phys.* **2**, 4.

Bruno, R., Carbone, V., Veltri, P., Pietropaolo, E., Bavassano, B.: 2001, Identifying intermittency events in the solar wind. *Planet. Space Sci.* **49**, 1201 – 1210.

Cranmer, S.R.: 2008, On competing models of coronal heating and solar wind acceleration: the debate in '08. arXiv e-prints No. 0804.3058.

Cranmer, S.R., van Ballegooijen, A.A.: 2005, On the generation, propagation, and reflection of Alfvén waves from the solar photosphere to the distant heliosphere. *Astrophys. J. Suppl. Ser.* **156**, 265 – 293. doi:10.1086/426507.

Fisk, L.A., Schwadron, N.A.: 2001, The behaviour of the open magnetic field of the Sun. *Astrophys. J.* **560**, 425 – 438.

Horbury, T.S., Burgess, D., Fränz, M., Owen, C.J.: 2001, Three spacecraft observations of solar wind discontinuities. *Geophys. Res. Lett.* **28**, 677 – 680. doi:10.1029/2000GL000121.

McComas, D.J., Bame, S.J., Barker, P., Feldman, W.C., Phillips, J.L., Riley, P., Griffee, J.W.: 1998, Solar wind electron proton alpha monitor (SWEPAM) for the advanced composition explorer. *Space Sci. Rev.* **86**, 563 – 612.

Owens, M.J., Crooker, N.U.: 2006, Coronal mass ejections and magnetic flux buildup in the heliosphere. *J. Geophys. Res.* **111**, 10104. doi:10.1029/2006JA011641.

Owens, M.J., Horbury, T.S., Arge, C.N.: 2010, Probing the large-scale topology of the heliospheric magnetic field using Jovian electrons. *Astrophys. J.* **714**, 1617 – 1623. doi:10.1088/0004-637X/714/2/1617.

Schwadron, N.A., McComas, D.J.: 2003, Solar wind scaling law. *Astrophys. J.* **599**, 1395 – 1403. doi:10.1086/379541.

Schwadron, N.A., McComas, D.J., DeForest, C.: 2006, Relationship between solar wind and coronal heating: scaling laws from solar X-rays. *Astrophys. J.* **642**, 1173 – 1176. doi:10.1086/501066.

Smith, C.W., L'Heureux, J., Ness, N.F., Acuna, M.H., Burlaga, L.F., Scheifele, J.: 1998, The ACE magnetic fields experiment. *Space Sci. Rev.* **86**, 613 – 632.

Verdini, A., Velli, M.: 2007, Alfvén waves and turbulence in the solar atmosphere and solar wind. *Astrophys. J.* **662**, 669 – 676. doi:10.1086/510710.

Viall, N.M., Spence, H.E., Kasper, J.: 2009, Are periodic solar wind number density structures formed in the solar corona? *Geophys. Res. Lett.* **36**, 23102. doi:10.1029/2009GL041191.

Wicks, R.T., Chapman, S.C., Dendy, R.O.: 2009, Spatial correlation of solar wind fluctuations and their solar cycle dependence. *Astrophys. J.* **690**, 734 – 742. doi:10.1088/0004-637X/690/1/734.